Published in final edited form as:
Virology. 2011 December 5; 421(1): 67–77. doi:10.1016/j.virol.2011.08.020.

Comparison of Differing Cytopathic Effects in Human Airway Epithelium of Parainfluenza Virus 5 (W3A), Parainfluenza Virus Type 3, and Respiratory Syncytial Virus

Liqun Zhang[a,*], **Peter L. Collins**[b], **Robert A. Lamb**[c], and **Raymond J. Pickles**[a,d]

[a]Cystic Fibrosis/Pulmonary Research and Treatment Center, University of North Carolina at Chapel Hill, Chapel Hill, North Carolina 27599, USA

[b]Laboratory of Infectious Diseases, National Institute of Allergy and Infectious Diseases, National Institutes of Health, Bethesda, Maryland 20892, USA

[c]Howard Hughes Medical Institute, Dept. of Molecular Biosciences, Northwestern University, Evanston, IL 60201-2138, USA

[d]Microbiology and Immunology, University of North Carolina at Chapel Hill, Chapel Hill, North Carolina 27599, USA

Abstract

Parainfluenza virus 5 (PIV5) infects a wide range of animals including dogs, pigs, cats, and humans; however, its association with disease in humans remains controversial. In contrast to parainfluenza virus 3 (PIV3) or respiratory syncytial virus (RSV), PIV5 is remarkably non-cytopathic in monolayer cultures of immortalized epithelial cells. To compare the cytopathology produced by these viruses in a relevant human tissue, we infected an in vitro model of human ciliated airway epithelium and measured outcomes of cytopathology. PIV5, PIV3 and, RSV all infected ciliated cells, and PIV5 and PIV3 infection was dependent on sialic acid residues. Only PIV5-infected cells formed syncytia. PIV5 infection resulted in a more rapid loss of infected cells by shedding of infected cells into the lumen. These studies revealed striking differences in cytopathology of PIV5 versus PIV3 or RSV and indicate the extent of cytopathology determined in cell-lines does not predict events in differentiated airway cells.

Keywords

Parainfluenza virus; respiratory syncytial virus; airway epithelium; cytopathic effect; viral pathogenesis; syncytia; ciliated cell shedding; viral persistence; multi-potent progenitor cells; 3-dimensional (3-D) image reconstruction

[*]Corresponding author: Liqun Zhang, Ph.D., UNC Cystic Fibrosis Center, 7021 Thurston-Bowles, CB# 7248, Chapel Hill, NC 27599-7248, Tel: +1-919-966-7044, Fax: +1-919-966-5178, liqun_zhang@med.unc.edu.

Introduction

PIV5, previously known as simian virus 5 (SV5), is an enveloped non-segmented negative strand RNA virus in the family *Paramyxoviridae. Paramyxoviridae* includes many important pathogens of humans and animals, including human respiratory syncytial virus (RSV), metapneumovirus, parainfluenza virus types 1-4 (PIV1-4), mumps virus, measles virus, Nipah/Hendra virus, rinderpest virus, and Newcastle disease virus (Karron and Collins, 2006). Most of these viruses have a limited host range. For example, humans are the only natural hosts for RSV, PIV1-3, human metapneumovirus, mumps, and measles viruses. In contrast, PIV5 has reportedly been isolated from a wide range of hosts including human, dog, pig, cat, hamster, and guinea pig (Chatziandreou et al., 2004).

PIV5 was first isolated in 1954 from primary monkey kidney cells but no evidence exists for natural infection of PIV5 in monkeys in the wild. However, monkeys in captivity quickly seroconvert suggesting susceptibility upon exposure (Hsiung, 1972; Hull, Minner, and Smith, 1956). PIV5 was identified as the causative agent of kennel cough, a respiratory illness of dogs (Binn et al., 1967; Cornwell et al., 1976). PIV5 has been isolated on numerous occasions from human tissues (Goswami et al., 1984) and neutralizing antibody against PIV5 was readily detectable in non-symptomatic human volunteers (Johnson, Capraro, and Parks, 2008). On the one hand, PIV5 has been suggested to be associated with various human diseases, although it remains controversial whether or not the virus naturally infects humans and whether or not it causes disease. On the other hand, it has been suggested that PIV5 is non-pathogenic in humans and could be a suitable vector for live viral vaccine applications (Tompkins et al., 2007). PIV5 is not routinely screened for in studies to identify viruses associated with human respiratory infections (Lee et al., 2007; Nolte et al., 2007), and large scale PIV5 surveillance has not been performed. Thus, the prevalence of PIV5 in humans and its impact on human health are currently unknown.

In typical monolayer cultures of immortalized cells, PIV5 causes a productive and persistent infection, but does not kill cells or shut off cellular RNA or protein synthesis (Choppin, 1964). This lack of cytopathology may be largely attributed to the multi-functional PIV5 V protein. The V protein functions primarily as an interferon antagonist by binding to MDA-5 to inhibit interferon induction (Andrejeva et al., 2004) and by binding to STAT1 resulting in its degradation and suppressing interferon signaling (Didcock et al., 1999). V also exhibits anti-apoptotic activity (Sun et al., 2004) and regulates viral replication and transcription to optimal levels to avoid detection of viral RNA by RIG-I, MDA5, toll like receptors, and protein kinase R that are involved in initiating innate immune responses (Lin et al., 2005). The ability of PIV5 to readily establish persistent, non-cytopathic infections in vitro may enable the establishment of persistent, nonpathogenic infections in vivo, although this remains speculative.

PIV5 infection of cell lines is mediated by negatively charged sialic acid residues present on cell surfaces (Scheid et al., 1972), although this is largely based on interactions in vitro with immortalized cells and erythrocytes. The human respiratory airway epithelium is decorated with abundant sialic acids at the lumenal surface (Thompson et al., 2006; Varki and Varki, 2007). Thus, airway epithelial cells are likely susceptible to PIV5 infection mediated by sialic acids, similar to PIV1-3 infection (Bartlett et al., 2008; Schaap-Nutt et al., 2010; Zhang et al., 2005). To validate this, we use an in vitro model of human airway epithelium (HAE), generated from human primary bronchial epithelial cells and differentiated at the air-liquid interface to reproduce the pseudostratified mucociliary epithelium of the airway as observed for the in vivo counterpart (Fulcher et al., 2005). Using the HAE model, we found that PIV5 infection of HAE occurs preferentially at the apical surface and is mediated by interaction with sialic acids. In comparison to RSV and PIV3, PIV5 was unexpectedly more

cytopathic, as characterized by enhanced shedding of infected cells and extensive formation of syncytia.

Results

PIV5 infection of the human airway epithelium (HAE) is preferably apical and sialic acid-dependent

To monitor PIV5 infection, we used a recombinant PIV5 (strain W3A) expressing GFP as an extra gene. Apical or basolateral surfaces of HAE were inoculated with PIV5 (2×10^6 PFU, MOI of 6) and incubated for 1 h at 37°C, and GFP fluorescence as an index of PIV5 infection was monitored over time. We observed that PIV5 infected HAE with a high efficiency from the apical surface, i.e., 66.9%, 69.7%, and 71.2% GFP+ cells en face at 1, 2, and 3 days pi respectively (Figure 1A). The lack of substantial increase in the numbers of infected cells over this period indicated that the infections were near the maximum. On the other hand, apical infection at a lower MOI (0.01) demonstrated robust viral spreading (Supplementary Figure 1). Upon basolateral inoculation, only a small number of cells (~1.5%) were infected at 1 day PI but the number of infected cells increased significantly to 20.2% and 34.7% at 2 and 3 days PI respectively, indicating robust propagation of PIV5 infection. Thus, similar to our previous reports with RSV and PIV3, the apical surface of HAE is more susceptible to initial infection with PIV5 than the basolateral surface; however, unlike RSV (Zhang et al., 2002) and PIV3 (Zhang et al., 2005), PIV5 exhibited increased tropism for the basolateral surfaces. Similar data has been obtained with PIV2, another rubulavirus, in an identical culture model (unpublished observation).

To test whether PIV5 infection in HAE was mediated by sialic acids, the apical surfaces of HAE were exposed to a broad spectrum neuraminidase (NA) from *Vibrio cholerae* (See Methods for details). The apical surfaces were then inoculated with PIV5 (MOI of 6), and GFP fluorescence visualized at 24 h PI (Figure 1B). We found that the NA treatment resulted in a large reduction of PIV5 infection from 67% to 28% of cells being GFP-positive (Figure 1C). In contrast, identical treatment of parallel cultures showed complete abrogation of PIV3 infection, as shown previously but no effect on RSV infection (Zhang et al., 2005). To verify that PIV5 infection is solely sialic acid-dependent, we carried out infections with PIV5, PIV3, and RSV on two CHO-derived cell lines, the wild type Pro-5 and sialic acid-deficient Lec2 cells. Monolayer cultures of Pro-5 and Lec2 cells were inoculated with equal titers of PIV5, PIV3, or RSV (MOI of 10), and the percentages of infected cells (GFP-positive) were quantified at 24 h PI (Figure 1D). Both cell types were equally susceptible to RSV infection, consistent with RSV infection being independent of sialic acid. In contrast, Lec2 cells – lacking sialic acid -- were completely resistant to infection by PIV5 or PIV3. This showed that PIV5, like PIV3, is completely dependent on sialic acid for infection in CHO cells, and possibly in HAE too.

PIV5 caused ciliated epithelial cell fusion

To further examine PIV5 infection of HAE, we monitored the fate of virus-infected cells over time. Replicate HAE cultures were inoculated with equal titers of PIV5, PIV3, or RSV (MOI of 6) and fixed 2, 4, and 7 days PI. To observe the morphology of infected cells, consecutive *z*-stacks (i.e., vertical stacking) of *x*-*y* (i.e., horizontal, or *en face*, plane) images were acquired with a Zeiss 510 Meta Laser Scanning Confocal Microscope, and *en face* views (*x*-*y*) were constructed by maximum *z*-projection (Figure 2A). Ciliated cells were visualized by immune-labeling with β-tubulin-IV antibody (red). The extensive co-localization of the cilia (red) and GFP-positive cells (shown in yellow) when viewed at 2 days PI suggested that all three viruses targeted ciliated cells. Examination of cultures at 4

and 7 days PI indicated a substantial decrease in staining with the tubulin-specific antibody, suggesting a loss of either ciliated cells or cilia themselves.

To observe the infected cells in the vertical dimension (*x*-*z*), we resliced the confocal stacks in *x*-*z* with ImageJ (Figure 2B). These images confirmed that all three viruses exclusively infected ciliated cells, and all caused the gradual loss of infected ciliated cells within the period of observation (7 days PI). The *x*-*z* sections also revealed virus-specific differences in the morphology of virus-infected cells. A number of the PIV5-infected cells appeared to have fused while in the epithelium to form GFP-positive multicellular bodies (syncytia), although the nuclei of the fused cells did not congregate together in a single cell body as commonly observed in syncytial formation in non-polarized cells. In contrast, similar cell fusions were absent from PIV3- or RSV-infected HAE. PIV3-infected ciliated cells retained typical columnar epithelial cell morphology. In contrast, RSV infection resulted in rounded ciliated cell morphology. To better capture the unique morphological features of infected ciliated cells, we performed three-dimensional (3D) reconstruction from confocal z-stack images (2 days PI) by volume rendering using Volocity software. The 3D structures of virus infected epithelial cells were rotated 360° and captured in a video format (Videos #1-3). The still images of the 3-D structures captured at 45° angle (with respect to planes of the epithelia) are shown in the print version. These data clearly demonstrated the fused columnar PIV5 infected cells, the non-fused columnar PIV3 infected cells, and the non-fused rounded RSV infected cells. Interestingly, the PIV5-infected cells appeared to have persisted in the epithelium during the time frame of this experiment (7 days), although staining for cilia was largely absent by 4 days PI. In contrast, the majority of PIV3- and RSV-infected cells disappeared from the epithelium by 7 days PI (Fig. 2B). It may be that the PIV5-infected cells persisted but shed their cilia; alternatively, the PIV5-infected ciliated cells may have been shed while the remaining non-ciliated cells were subsequently infected by PIV5. To reveal these potential differences, we next investigated the fates of infected ciliated cells.

PIV5 caused greater loss of ciliated epithelial cells than PIV3 or RSV

To determine the consequences of viral infection of HAE, we examined histological sections at 3 days PI, the day after peak viral infections. For mock-inoculated HAE, the typical pseudostratified morphology with abundant ciliated cells was observed (Figure 3A). Occasionally, detached cells were observed on the apical surface, indicative of homeostatic cell turnover. In contrast, for PIV5-infected HAE, ciliated cells were largely absent by this time point, 3 days PI. Furthermore, a greater number of detached cells were present on apical surfaces suggesting shedding of infected cells into the lumenal compartment. This observation was strengthened by noting the height of the epithelium (thickness), again suggesting significant loss of cells from the epithelium inoculated with PIV5. At these earlier time-points, PIV3-infected HAE exhibited few obvious changes compared to mock-infected cultures. RSV infection led to the rounding of ciliated cells and to an uneven lumenal surface (Figures 3A and 2B).

To compare cell loss after virus infection, the numbers of cells remaining per unit length of the histological sections were quantified (Figure 3B). These data revealed that PIV5-infected HAE contained approximately one half of the cell numbers for mock-infected HAE, indicating a significant and substantial loss of the cells from HAE by 3 days PI. In comparison, PIV3 infection of HAE resulted in a loss of 20% of cells whereas, RSV infection resulted in no significant loss of cells compared to mock-inoculated HAE. Thus, comparisons of cell loss among these three viruses that all target ciliated cells shows PIV5 caused the greatest loss of ciliated cells by 3 days PI.

Airway epithelial cell proliferation rates were not affected by viral infection

Since PIV5 and PIV3 caused significant loss of epithelial cells from HAE, we tested whether the loss of epithelial cells stimulated cellular proliferation to initiate the repair of the infected epithelium. To quantify the numbers of dividing cells, HAE cultures, mock-inoculated or inoculated with PIV5, PIV3, or RSV (apical, MOI of 6), were exposed at 3 days PI to 5-bromo-2-deoxyuridine (BrdU) for 6 hrs, to identify dividing cells. In mock-inoculated cells BrdU-label was predominately incorporated into the nuclei (dark brown) of basal cells (Figure 4A), indicating the plasticity of this epithelial cell progenitor population. Proliferation rates were determined by measuring the number of dividing cells per unit length of epithelium. These rates were found to be comparable among HAE infected with PIV5, PIV3, or RSV, or mock-inoculated (Figure 4B). While PIV5 appeared to modestly increase the cellular proliferation rate, and PIV3 appeared to modestly reduce the rate, neither change reached statistical significance ($p > 0.05$). Therefore, infections by PIV5, PIV3, or RSV did not significantly alter the rate of cellular proliferation in HAE.

PIV5 is associated with greater cell shedding than PIV3 and RSV in human airway epithelium in vitro

We have previously shown PIV3-infected ciliated cells are extruded onto the apical surface of HAE likely by cell detachment and expulsion from the epithelium (Zhang et al., 2009). To compare the extent of shedding of infected cells after PIV5, PIV3 or RSV infection, we harvested the apical washes containing extruded epithelial cells from HAE inoculated with viruses. To identify shed cells, apical washes were cyto-centrifuged onto glass slides and stained with Giemsa. Representative photomicrographs of samples harvested at 1, 4, and 7 days PI are shown in Figure 5. As expected, ciliated cells were the predominant cell-type present in the apical wash. While lower numbers of ciliated cells were identified in washes from mock-inoculated HAE, significantly more cells were present in apical washes from HAE infected with any of the viruses. Notably, shed cells from PIV5-infected HAE were often observed in large clumps, consistent with fused infected cells (Figure 2). In contrast, shed cells from PIV3- and RSV-infected HAE, were observed as individual cells.

To quantify the differences in cell shedding after infection by different viruses, a quantitative assay for the amount of dsDNA shed into the apical washes was used. This assay enables the dsDNA amounts to be used as an index for the numbers of cells shed into the luminal compartment of HAE, and the dsDNA amounts correlate well with the numbers of cells shed from the epithelium quantitated by histological analysis (data not shown). Apical washes were freeze-thawed three times to release nuclear dsDNA, and the total amounts of dsDNA present in spin-cleared supernatants quantified with the PicoGreen dsDNA reagent (see Methods for details). As shown in Figure 6A, PIV5 caused early and significant increase in cell shedding even at 1 day PI, whereas PIV3 and RSV infection at this time-point did not increase cell shedding above that measured for mock-inoculated cultures. Overall, there was a delay in cell shedding after PIV5 infection with PIV5-mediated cell shedding peaking at 2 days PI and PIV3-mediated or RSV-mediated cell shedding peaking at 3 days PI. Thus, cell shedding in response to PIV5 infection occurred earlier and was more severe than in response to PIV3 or RSV.

To establish whether cell shedding led to a loss of epithelium barrier integrity, we next measured the transepithelial electrical resistance (TEER) in mock and virus infected HAE daily for up to 8 days PI (Figure 6B). No significant changes in TEER in any of the cultures at 1 and 2 days PI were observed, indicating an intact epithelial barrier. However, the TEER in PIV5-infected HAE dropped significantly at 3 days PI, one day after the peak of cell shedding with this virus (Figure 6A). This suggested that a compromise in epithelial integrity coincided with epithelial cell shedding. PIV3- or RSV-infected HAE also showed

significant reduction in TEER compared to mock-inoculated cultures one day after peak cell shedding (4 days PI). Thus, virus-induced decreases in TEER are likely a direct consequence of virus-induced cell shedding. Compared to PIV3 and RSV, PIV5 more rapidly and more robustly caused cell shedding of the epithelium.

As part of the innate immune response, epithelial cells produce interferon and other anti-viral cytokines upon viral infection. Interferon, however, has been suggested to induce the death of virus infected epithelial cells (Schuhmann et al., 2010). To investigate whether cell shedding in response to virus infection is linked to interferon production of the epithelial cells, we compared the amounts of type I interferon produced by HAE infected with PIV5, PIV3, and RSV. As interferon secretion from HAE is non-polarized (data not shown), we assessed interferon levels secreted into the basolateral compartment from mock and virus inoculated HAE at 1, 2, 3, and 4 days PI. Type I interferon was measured using an interferon bioassay (see Methods). As predicted, type I interferon was induced by all viruses with PIV5 (W3A) inducing the least amount of interferon among the three viruses, and PIV3 inducing almost twice as much interferon than PIV5 or RSV (except at 4 days PI) (Figure 6C). The difference in interferon induction was not due to how viruses were prepared, as the UV-inactivated viruses induced no interferon (data not shown). As PIV5 infection results in more rapid and robust shedding of the infected cells, the observation this virus produces the least interferon would suggest interferon is not the causative factor for mediating epithelial cell shedding in HAE. In contrast to interferon, we found PIV5 induced the expression of other cyto/chemokines at comparable levels to those induced by PIV3 or RSV infection (Supplementary Figure 4).

Discussion

The HAE model closely resembles the authentic human airway epithelium and provides a useful in vitro system for evaluating the replication and cytopathology of respiratory viruses in the absence of the confounding factors of adaptive and cell-mediated immune responses. Using the HAE model, we have demonstrated that -- in contrast to a common misconception based on observations using standard monolayer cell cultures -- RSV does not cause syncytial formation in the airway epithelium, consistent with the limited histopathologic findings from RSV-infected humans (Zhang et al., 2002). Furthermore, the growth kinetics and attenuation phenotypes of several attenuated PIV2 strains in HAE paralleled those in non-human primates in vivo, indicating a close correspondence with this in vitro model (Schaap-Nutt et al., 2010). In the present study, we used the HAE model to evaluate infection by the paramyxovirus PIV5. PIV5 is unique among related viruses for its apparent low cytotoxicity in cell monolayers, even though PIV5 infects many cell lines from various species. Using the HAE model, we showed that PIV5 caused greater shedding of virus-infected ciliated cells compared to the common human respiratory paramyxovirus pathogens PIV3 and RSV that were evaluated in parallel. Although PIV5 appeared to preferentially infect ciliated cells, it subsequently caused fusion between the infected ciliated cells with surrounding cells. This fusogenic property of PIV5 was unique amongst the paramyxoviruses that we have tested to date, including RSV, PIV1, PIV2, and PIV3 (Bartlett et al., 2008; Schaap-Nutt et al., 2010; Zhang et al., 2005; Zhang et al., 2002). While PIV5, PIV3, and RSV are all capable of causing syncytia in standard monolayer cell lines, only PIV5 caused syncytia formation in HAE. The reason for this difference is unknown and is under investigation.

The viral strains used are critically important when interpreting experimental results. We chose the W3A strain of PIV5, as among about a dozen of PIV5 strains known so far, the W3A was the first isolated and is the best characterized so far. To date W3A remains the only strain whose genome has been completely sequenced. It would be interesting to test a

less fusogenic strain such as SER (Tong et al., 2002), whose fusion protein has a 22 amino acid extension at the cytoplasmic domain. Nonetheless, no strains of PIV5 (including W3A) are linked with human diseases. Our observation that W3A is more cytopathic than PIV3 and RSV is unexpected, highlighting the need for further studies in vivo in an appropriate animal model. The RSV strain (A2) used in our study is a recombinant version of a laboratory strain; its sequence is nearly identical to the original clinical isolate. Like the clinical isolate, the recombinant virus caused respiratory tract disease in chimpanzees (unpublished observations). The PIV3 virus is a recombinant version of JS strain, derived from a clinical isolate rather than a laboratory strain. The parental virus used at the Laboratory of Infectious Diseases, National Institutes of Health (Bethesda, MD) from which the recombinant virus was derived, replicated efficiently in chimpanzees and caused disease (Clements et al., 1991).

We demonstrated that PIV5 infection was sialic acid-dependent. The residual PIV5 infection after NA treatment indicated significant amounts of PIV5-binding molecules were not removed by *V. cholerae* NA, even though the same treatment removed all of the PIV3-binding sialic acids. This could be explained by the observation that PIV5 recognizes a broader spectrum of sialic acid structures including the ganglio and the neolacto series, while PIV3 binds only the neolacto series of sialic acids (Suzuki et al., 2001). Alternatively, PIV5 may bind to completely different yet un-identified molecules on HAE. We also determined that sulfated polysaccharides did not support PIV5 infection in HAE. Specifically, we found that mixing PIV5 with either fucoidan (Supplementary Figure 2) or heparan sulfate (data not shown) did not affect the efficiency of infection in HAE, whereas RSV infection was inhibited by fucoidan in a dose dependent manner. Taken together, HAE may express a broader variety of sialic acids or other PIV5 receptors than immortalized cell lines, and PIV5 may recognize a broader range of receptors than PIV3, including ones that are resistant to *V. cholerae* NA. Nonetheless, PIV5 infection of HAE is most likely dependent on sialic acid residues.

Viral infection significantly increased the shedding of epithelial cells compared to mock-infected HAE (Figure 6A). This could occur in two different scenarios: (1) virus-induced cell death followed by exclusion from the epithelium or (2) host cell-mediated acceleration of the shedding of viral infected cells (still alive) as a host defense mechanism to clear virus infected cells from the epithelium. The second scenario was found to be more likely based on a trypan blue exclusion assay (data not shown), which indicated that virus-infected cells in the epithelium, regardless of their shapes, retained plasma membrane integrity, suggesting that they remained viable. Compared to the robust cytopathology in HAE observed after influenza virus infection (Thompson et al., 2006; Zhang et al., 2002), the shedding of virus-infected cells in this study resulted in only moderate disruption to the epithelial integrity, with PIV5 being more disruptive than PIV3 or RSV.

The BrdU incorporation assay demonstrated that the surface epithelial cells (both ciliated and mucous cells) in HAE did not rapidly divide after virus infection, suggesting a terminally differentiated state. Trans-differentiation of ciliated cells to mucous cells after virus infection has been reported (Tyner et al., 2006) but was not observed in the present study. In contrast, we found that basal epithelial cells in HAE did incorporate BrdU, indicative of cell division. Furthermore, Over time, the proliferating basal cells migrated and differentiated into surface epithelial cells, or remained as a component of the basal cell layer (self-renewal) (Supplementary Figure 3). We had anticipated that the rate of basal cell proliferation might increase upon viral infection in HAE, in order to compensate for the increased cell shedding. However, the rate of basal cell division in HAE remained unchanged by infection by any of the viruses (Figure 4). As a consequence, viral infection,

especially by PIV5, resulted in a “thinning” of the epithelium and a progressive loss of barrier integrity.

PIV5 infection in certain immortalized cell lines demonstrates a notable lack of cytopathology and in some cases viral persistence. A human gastric epithelial adenocarcinoma cell line (AGS) was reported to be persistently infected with PIV5 (Young et al., 2007). Recently, a human naso-pharyngeal carcinoma cell line (C666-1) was found to harbor persistent PIV5 infection (Personal communication, Nancy Raab-Traub, UNC). Interestingly, both cell lines showed unusually high percentages of cell death during routine passages (unpublished observations), suggesting there was a cost associated with accommodating PIV5 replication. PIV5 together with PIV2 and a strain of Sendai virus (SeVpi) were demonstrated to exhibit high efficiencies in establishing persistent viral infections in cell lines (Ito et al., 2009). These studies suggest PIV5 might persist in vivo, although this has never been demonstrated.

PIV5 is very permissive in its ability to infect immortalized cell lines in vitro. It also reportedly has been recovered from diverse mammalian hosts, including dogs, pigs and humans. The present study indicated that PIV5 utilizes a wider range of surface sialic acid species as receptor, which might confer increased host range. PIV5 is a common agent of respiratory tract disease in dogs, but its natural history in other species is unclear. In particular, as noted, PIV5 has widely been speculated to be a common agent of infection in humans and a potential agent in a number of human diseases, but this remains unclear (Introduction). A countervailing opinion is that PIV5 infection of humans likely is benign, and that PIV5 might be suitable as a vaccine vector for human use. The present study showed that PIV5 infection of HAE shared some characteristics with that of the common human pathogens RSV and the PIVs, such as tropism for the surface ciliated epithelial cells. Given the wide speculation that PIV5 infection might be persistent or benign, we had anticipated that PIV5 would be less cytopathic in HAE than RSV and the human PIVs, which can cause serious respiratory tract disease in humans. For example, Persistent infection is often associated with reduced viral pathogenesis (Rima and Martin, 1976) and decreased fusogenic activity of virus proteins (Sarmiento et al., 2009). However, the converse was observed: in contrast to RSV and the human PIVs, PIV5 was substantially fusogenic and invasive, caused increased cell shedding, resulted in a thinning of the epithelium, and caused a greater compromise to epithelial integrity. This illustrates the uncertainty of predicting pathogenesis and persistence based on properties observed in monolayer cultures of immortalized cells. HAE cultures also represent an in vitro system, but they recreate a mucociliary pseudostratified tissue that closely resembles authentic airway epithelium in structure and function, and uniquely provide an evaluation of direct viral cytopathology in the absence of immune destruction.

In summary, we showed PIV5 efficiently infects human ciliated airway epithelial cells. Infection was mediated primarily by surface sialic acid residues and was associated with greater cytopathology than PIV3 or RSV assayed directly in parallel. This study shows that primary human epithelial cells are efficiently infected by PIV5, consistent with the possibility that humans might be a permissive host for the virus. However, the increased pathogenesis observed in HAE cultures – compared to the common viral agents of respiratory tract disease RSV and the human PIVs – raises the possibility that PIV5 infection of the respiratory tract might not be benign. Future in vivo studies will be required to shed light on these questions.

Material and Methods

Cells and viruses

Human lung carcinoma cells A549 (ATCC# CCL-185) were grown in Dulbecco's Modified Eagle Medium (DMEM) supplemented with 10% fetal bovine serum (FBS) and penicillin-streptomycin (Pen-Strep). CHO derivatives Pro-5 (ATCC# CRL-1781) and Lec2 (ATCC# CRL-1736) cells were grown in Minimum Essential Medium (MEM) α supplemented with 10% FBS, 40 μg/ml proline, and Pen-Strep. The human airway epithelial cell culture model (HAE) was generated as described previously (Fulcher et al., 2005). Recombinant PIV5 was derived from W3A strain and contained a GFP reporter gene between HN and L (He et al., 1997). RSV (Hallak et al., 2000) and PIV3 (Zhang et al., 2005) are recombinant GFP-expressing viruses based on the RSV A2 and PIV3 JS strains respectively. Note all viruses used in these studies express GFP.

Enzymatic removal of sialic acids from HAE with neuraminidase (NA) treatment

The sialic acid residues on the apical surface of HAE were removed by treatment with NA from *Vibro cholerae* (Sigma N-6514). The apical surface of HAE was rinsed three times with PBS to remove accumulated mucus. NA, diluted with serum-free medium to a final concentration of 200 mU/ml, was inoculated on the apical surface of HAE and incubated for 3 h at 37°C, followed by NA removal and washing with PBS. Viral infections were carried out immediately after NA treatment.

Identification of dividing cells by BrdU labeling and immunohistochemical staining

Replicate HAE cultures were mock-infected or infected with virus (MOI of 6), incubated for 3 days, and labeled by incubation with 10 μM 5-bromo-2-deoxyuridine (BrdU) (Invitrogen) for 6 h followed by fixation with 4% paraformaldehyde (PFA) at 4°C overnight. The fixed HAE was then paraffin-embedded and sectioned (5 μm). BrdU-labeled nuclei were immunostained using a Zymed BrdU Staining Kit (Invitrogen) (shown in dark brown) and cell nuclei counter-stained with hematoxylin (shown in blue).

Cytology of shed cells

Phenol red-free serum-free DMEM was added to the apical surfaces of mock or virus-infected HAE cultures (0.4 ml per 12 mmØ culture) at the indicated days PI and allowed to incubate for 30 min before being harvested with a pipette. Half of the solution (0.2 ml) was used for measuring dsDNA content (see below) and the rest (0.2 ml) was cyto-centrifuged at 700× rpm for 4 min onto glass slides using a StatSpin CytoFuge 2 (Iris Sample Processing). The slides were air-dried, fixed in 4% PFA, and stained with Giemsa by the UNC CF Center Histology Core.

Photomicrographic image capture and processing

Fluorescence and bright field photomicrographs were captured by using a Leica DMIRB Inverted Fluorescent Microscope equipped with a Q-Imaging Retiga 1300 CCD camera. Confocal *x*-*z* images and *z*-stacks were acquired with a Zeiss 510 Meta Laser Scanning Confocal Microscope. *X*-*z* reslicing of the confocal *z*-stack was performed with the ImageJ software (NIH), and 3D image reconstructions by volume rendering were carried out with Volocity software (Improvision/Perkin Elmer). Other image processing and calculations were performed with Adobe Photoshop (Adobe).

Quantification of dsDNA for cell shedding analysis

The total amount of dsDNA present in the apical washes of HAE were quantified in 96-well plate format using a Quant-iT PicoGreen dsDNA Kit (Invitrogen #P11496). Briefly, washes

from HAE cells were freeze-and-thawed three times to release nuclear dsDNA, and cellular debris was removed by centrifugation (2,500*g* for 10 min). The supernatants were then diluted five fold with TE buffer (10 mM Tris-Cl, pH 7.5, 1 mM EDTA) in 96-well plates followed by the addition of diluted PicoGreen dsDNA reagent. Each sample was run in duplicate, and fluorescence signals were read with a Tecan Infinite M1000 Microplate Reader (Ex/Em 480/520 nm).

Type I interferon (IFN) bioassay

Type I IFN levels in cell culture supernatants were determined by a CPE inhibition bioassay using A549 cells and encephalomyocarditis virus (EMCV) (ATCC# VR-129B) as described previously (Shabman, Rogers, and Heise, 2008). Briefly, serial two-fold dilutions of test supernatants in duplicate were cultured with A549 cells (2×10^4 per well in 96-well plates) for 24 h. Cells were then infected with EMCV at a MOI of 5; 24 h later the plates were stained for attached cells with 0.1% crystal violet/20% methanol. The bioassay plates were scored for 50% CPE as an indicator of IFN concentration. Each plate also contained an internal IFN standard, the recombinant human IFN-β (Invitrogen PHC4244), which had been calibrated against the NIH human IFN-β reference standard (Gb23-902-531). The deduced IFN concentrations in test samples were expressed as international units (IU) per ml.

Statistics

Statistical analyses, including student's *t* test and one-way analysis of variance (ANOVA) (Holm-Sidak method), were performed using SigmaStat 3.11 (Systat Software Inc). Statistical significance was defined as $p < 0.05$ unless otherwise noted.

Supplementary Material

Refer to Web version on PubMed Central for supplementary material.

Acknowledgments

We thank the UNC CF Center Tissue Procurement and Cell Culture Core, the Michael Hooker Microscopy Core Facility, and Histology Core Facilities. We also thank Dr. Jarrod Johnson (UNC Gene Therapy Center) for sharing the Pro-5 and Lec2 cells.

This work was supported in part by the Cystic Fibrosis Foundation (Zhang03I0) and the National Institutes of Health (R01 HL77844, P01 HL051818, P30 DK065988, P30 DK047757, and R01 AI23173). PLC was supported by the NIAID Intramural Program. RAL is an Investigator of the Howard Hughes Medical Institute. Sources of funding played no roles in study design, in the collection, analysis, and interpretation of the data, in the writing of the report, or in the decision to submit the paper for publication.

References

Andrejeva J, Childs KS, Young DF, Carlos TS, Stock N, Goodbourn S, Randall RE. The V proteins of paramyxoviruses bind the IFN-inducible RNA helicase, mda-5, and inhibit its activation of the IFN-beta promoter. Proc Natl Acad Sci U S A. 2004; 101(49):17264–9. [PubMed: 15563593]

Bartlett EJ, Hennessey M, Skiadopoulos MH, Schmidt AC, Collins PL, Murphy BR, Pickles RJ. Role of interferon in the replication of human parainfluenza virus type 1 wild type and mutant viruses in human ciliated airway epithelium. J Virol. 2008; 82(16):8059–70. [PubMed: 18524813]

Binn LN, Eddy GA, Lazar EC, Helms J, Murnane T. Viruses recovered from laboratory dogs with respiratory disease. Proc Soc Exp Biol Med. 1967; 126(1):140–5. [PubMed: 4294430]

Chatziandreou N, Stock N, Young D, Andrejeva J, Hagmaier K, McGeoch DJ, Randall RE. Relationships and host range of human, canine, simian and porcine isolates of simian virus 5 (parainfluenza virus 5). J Gen Virol. 2004; 85(Pt 10):3007–16. [PubMed: 15448364]

Choppin PW. Multiplication Of A Myxovirus (Sv5) With Minimal Cytopathic Effects And Without Interference. Virology. 1964; 23:224–33. [PubMed: 14192298]

Clements ML, Belshe RB, King J, Newman F, Westblom TU, Tierney EL, London WT, Murphy BR. Evaluation of bovine, cold-adapted human, and wild-type human parainfluenza type 3 viruses in adult volunteers and in chimpanzees. J Clin Microbiol. 1991; 29(6):1175–82. [PubMed: 1650789]

Cornwell HJ, McCandlish IA, Thompson H, Laird HM, Wright NG. Isolation of parainfluenza virus SV5 from dogs with respiratory disease. Vet Rec. 1976; 98(15):301–2. [PubMed: 179186]

Didcock L, Young DF, Goodbourn S, Randall RE. The V protein of simian virus 5 inhibits interferon signalling by targeting STAT1 for proteasome-mediated degradation. J Virol. 1999; 73(12):9928–33. [PubMed: 10559305]

Fulcher ML, Gabriel S, Burns KA, Yankaskas JR, Randell SH. Well-differentiated human airway epithelial cell cultures. Methods Mol Med. 2005; 107:183–206. [PubMed: 15492373]

Goswami KK, Cameron KR, Russell WC, Lange LS, Mitchell DN. Evidence for the persistence of paramyxoviruses in human bone marrows. J Gen Virol. 1984; 65(Pt 11):1881–8. [PubMed: 6389770]

Hallak LK, Collins PL, Knudson W, Peeples ME. Iduronic acid-containing glycosaminoglycans on target cells are required for efficient respiratory syncytial virus infection. Virology. 2000; 271(2): 264–75. [PubMed: 10860881]

He B, Paterson RG, Ward CD, Lamb RA. Recovery of infectious SV5 from cloned DNA and expression of a foreign gene. Virology. 1997; 237(2):249–60. [PubMed: 9356337]

Hsiung GD. Parainfluenza-5 virus. Infection of man and animal. Prog Med Virol. 1972; 14:241–74. [PubMed: 4338190]

Hull RN, Minner JR, Smith JW. New viral agents recovered from tissue cultures of monkey kidney cells. I. Origin and properties of cytopathogenic agents S.V.1, S.V.2, S.V.4, S.V.5, S.V.6, S.V.11, S.V.12 and S.V.15. Am J Hyg. 1956; 63(2):204–15. [PubMed: 13302209]

Ito M, Yamakawa I, Nishio M, Tsurudome M, Kawano M, Komada H, Ito Y. A quantitative method for analyzing establishing-efficiency of persistent viral infection. Microbiol Immunol. 2009; 53(5): 259–65. [PubMed: 19457166]

Johnson JB, Capraro GA, Parks GD. Differential mechanisms of complement-mediated neutralization of the closely related paramyxoviruses simian virus 5 and mumps virus. Virology. 2008; 376(1): 112–23. [PubMed: 18440578]

Karron, RA.; Collins, PL. Parainfluenza viruses. In: Knipe, DM.; Howley, PM., editors. Fields' virology. 5. Vol. 1.2. Lippincott Williams & Wilkins; Philadelphia, PA: 2006.

Lee WM, Grindle K, Pappas T, Marshall DJ, Moser MJ, Beaty EL, Shult PA, Prudent JR, Gern JE. High-throughput, sensitive, and accurate multiplex PCR-microsphere flow cytometry system for large-scale comprehensive detection of respiratory viruses. J Clin Microbiol. 2007; 45(8):2626–34. [PubMed: 17537928]

Lin Y, Horvath F, Aligo JA, Wilson R, He B. The role of simian virus 5 V protein on viral RNA synthesis. Virology. 2005; 338(2):270–80. [PubMed: 15950997]

Nolte FS, Marshall DJ, Rasberry C, Schievelbein S, Banks GG, Storch GA, Arens MQ, Buller RS, Prudent JR. MultiCode-PLx system for multiplexed detection of seventeen respiratory viruses. J Clin Microbiol. 2007; 45(9):2779–86. [PubMed: 17596361]

Rima RK, Martin SJ. Persistent infection of tissue culture cells by RNA viruses. Med Microbiol Immunol. 1976; 162(2):89–119. [PubMed: 934025]

Sarmiento RE, Arias CF, Mendez E, Gomez B. Characterization of a persistent respiratory syncytial virus showing a low-fusogenic activity associated to an impaired F protein. Virus Res. 2009; 139(1):39–47. [PubMed: 19014983]

Schaap-Nutt A, Scull MA, Schmidt AC, Murphy BR, Pickles RJ. Growth restriction of an experimental live attenuated human parainfluenza virus type 2 vaccine in human ciliated airway epithelium in vitro parallels attenuation in African green monkeys. Vaccine. 2010; 28(15):2788–98. [PubMed: 20139039]

Scheid A, Caliguiri LA, Compans RW, Choppin PW. Isolation of paramyxovirus glycoproteins. Association of both hemagglutinating and neuraminidase activities with the larger SV5 glycoprotein. Virology. 1972; 50(3):640–52. [PubMed: 4118317]

Schuhmann D, Godoy P, Weiss C, Gerloff A, Singer MV, Dooley S, Bocker U. Interfering with interferon-gamma signalling in intestinal epithelial cells: selective inhibition of apoptosis-maintained secretion of anti-inflammatory interleukin-18 binding protein. Clin Exp Immunol. 2010; 163(1):65–76. [PubMed: 21078084]

Shabman RS, Rogers KM, Heise MT. Ross River virus envelope glycans contribute to type I interferon production in myeloid dendritic cells. J Virol. 2008; 82(24):12374–83. [PubMed: 18922878]

Sun M, Rothermel TA, Shuman L, Aligo JA, Xu S, Lin Y, Lamb RA, He B. Conserved cysteine-rich domain of paramyxovirus simian virus 5 V protein plays an important role in blocking apoptosis. J Virol. 2004; 78(10):5068–78. [PubMed: 15113888]

Suzuki T, Portner A, Scroggs RA, Uchikawa M, Koyama N, Matsuo K, Suzuki Y, Takimoto T. Receptor specificities of human respiroviruses. J Virol. 2001; 75(10):4604–13. [PubMed: 11312330]

Thompson CI, Barclay WS, Zambon MC, Pickles RJ. Infection of human airway epithelium by human and avian strains of influenza a virus. J Virol. 2006; 80(16):8060–8. [PubMed: 16873262]

Tompkins SM, Lin Y, Leser GP, Kramer KA, Haas DL, Howerth EW, Xu J, Kennett MJ, Durbin RK, Durbin JE, Tripp R, Lamb RA, He B. Recombinant parainfluenza virus 5 (PIV5) expressing the influenza A virus hemagglutinin provides immunity in mice to influenza A virus challenge. Virology. 2007; 362(1):139–50. [PubMed: 17254623]

Tong S, Li M, Vincent A, Compans RW, Fritsch E, Beier R, Klenk C, Ohuchi M, Klenk HD. Regulation of fusion activity by the cytoplasmic domain of a paramyxovirus F protein. Virology. 2002; 301(2):322–333. [PubMed: 12359434]

Tyner JW, Kim EY, Ide K, Pelletier MR, Roswit WT, Morton JD, Battaile JT, Patel AC, Patterson GA, Castro M, Spoor MS, You Y, Brody SL, Holtzman MJ. Blocking airway mucous cell metaplasia by inhibiting EGFR antiapoptosis and IL-13 transdifferentiation signals. J Clin Invest. 2006; 116(2):309–21. [PubMed: 16453019]

Varki NM, Varki A. Diversity in cell surface sialic acid presentations: implications for biology and disease. Lab Invest. 2007; 87(9):851–7. [PubMed: 17632542]

Young DF, Carlos TS, Hagmaier K, Fan L, Randall RE. AGS and other tissue culture cells can unknowingly be persistently infected with PIV5; a virus that blocks interferon signalling by degrading STAT1. Virology. 2007; 365(1):238–40. [PubMed: 17509637]

Zhang L, Bukreyev A, Thompson CI, Watson B, Peeples ME, Collins PL, Pickles RJ. Infection of ciliated cells by human parainfluenza virus type 3 in an in vitro model of human airway epithelium. J Virol. 2005; 79(2):1113–24. [PubMed: 15613339]

Zhang L, Button B, Gabriel SE, Burkett S, Yan Y, Skiadopoulos MH, Dang YL, Vogel LN, McKay T, Mengos A, Boucher RC, Collins PL, Pickles RJ. CFTR delivery to 25% of surface epithelial cells restores normal rates of mucus transport to human cystic fibrosis airway epithelium. PLoS Biol. 2009; 7(7):e1000155. [PubMed: 19621064]

Zhang L, Peeples ME, Boucher RC, Collins PL, Pickles RJ. Respiratory syncytial virus infection of human airway epithelial cells is polarized, specific to ciliated cells, and without obvious cytopathology. J Virol. 2002; 76(11):5654–66. [PubMed: 11991994]

Abbreviations

Ap	apical
BL	basolateral
BrdU	5-bromo-2-deoxyuridine
CPE	cytopathic effect
EMCV	encephalomyocarditis virus
GFP	green fluorescent protein
HAE	human airway epithelial cells

H&E	hematoxylin and eosin
IFN	interferon
MOI	multiplicity of infection
NA	neuraminidase
PFA	paraformaldehyde
PI	post inoculation
PIV3	parainfluenza virus type 3
PIV5	parainfluenza virus type 5
qRT-PCR	quantitative real-time PCR
RSV	respiratory syncytial virus
SEM	standard error of mean
TEER	trans-epithelial electrical resistance

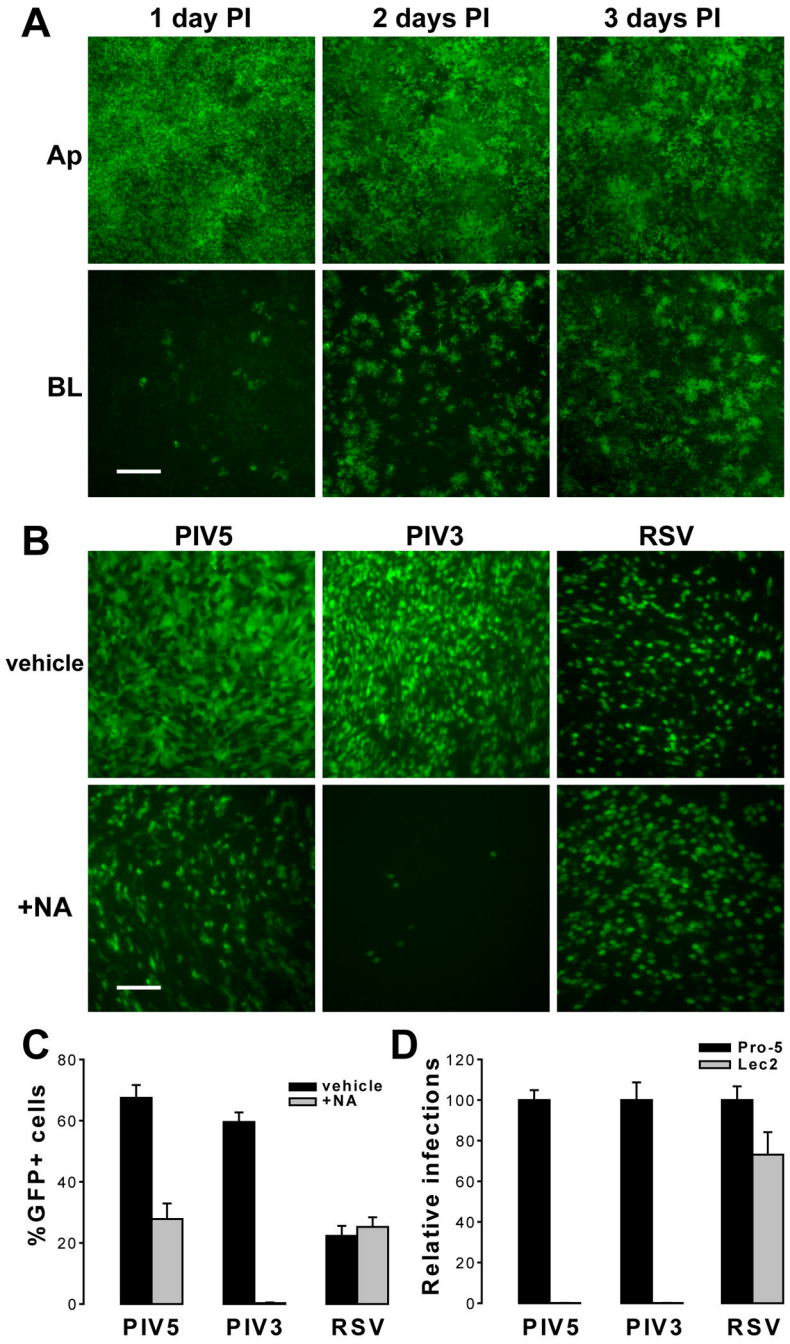

Figure 1. PIV5 infection of human airway epithelium is polarized and sialic acid-dependent

(**A**) Differentiated human airway epithelial (HAE) cell cultures were inoculated with equal amounts of PIV5 expressing GFP (2×10^6 PFU per cm^2 epithelia; MOI of 6) at either the apical (Ap) or basolateral (BL) surface. GFP expression as an indicator of viral infection was monitored over time, and representative fluorescence photomicrographs (*en face*, or x-y plane) were captured at 1, 2, and 3 days post inoculation (PI). Scale bar represents 200 μm. (**B**) HAE cultures were treated on the apical surface with either vehicle only or with neuraminidase (NA) from *V. cholerae* and then were inoculated with 2×10^6 PFU (per cm^2 epithelia; MOI of 6) of PIV5, PIV3, or RSV (all expressing GFP). Fluorescence photomicrographs were taken *en face* at 24 h PI (scale bar = 50 μm). The percentages of

GFP-positive cells in images of five random fields for each treatment were quantified with ImageJ, and the means ± SEM are shown in (**C**). (**D**) Wild type Pro-5 and sialic-acid-deficient Lec2 cell monolayers were infected with PIV5, PIV3, or RSV (MOI of 10). GFP expression was quantified at 24 h PI and expressed as normalized to Pro-5 cells as 100% (± SEM, $n = 6$ random fields each).

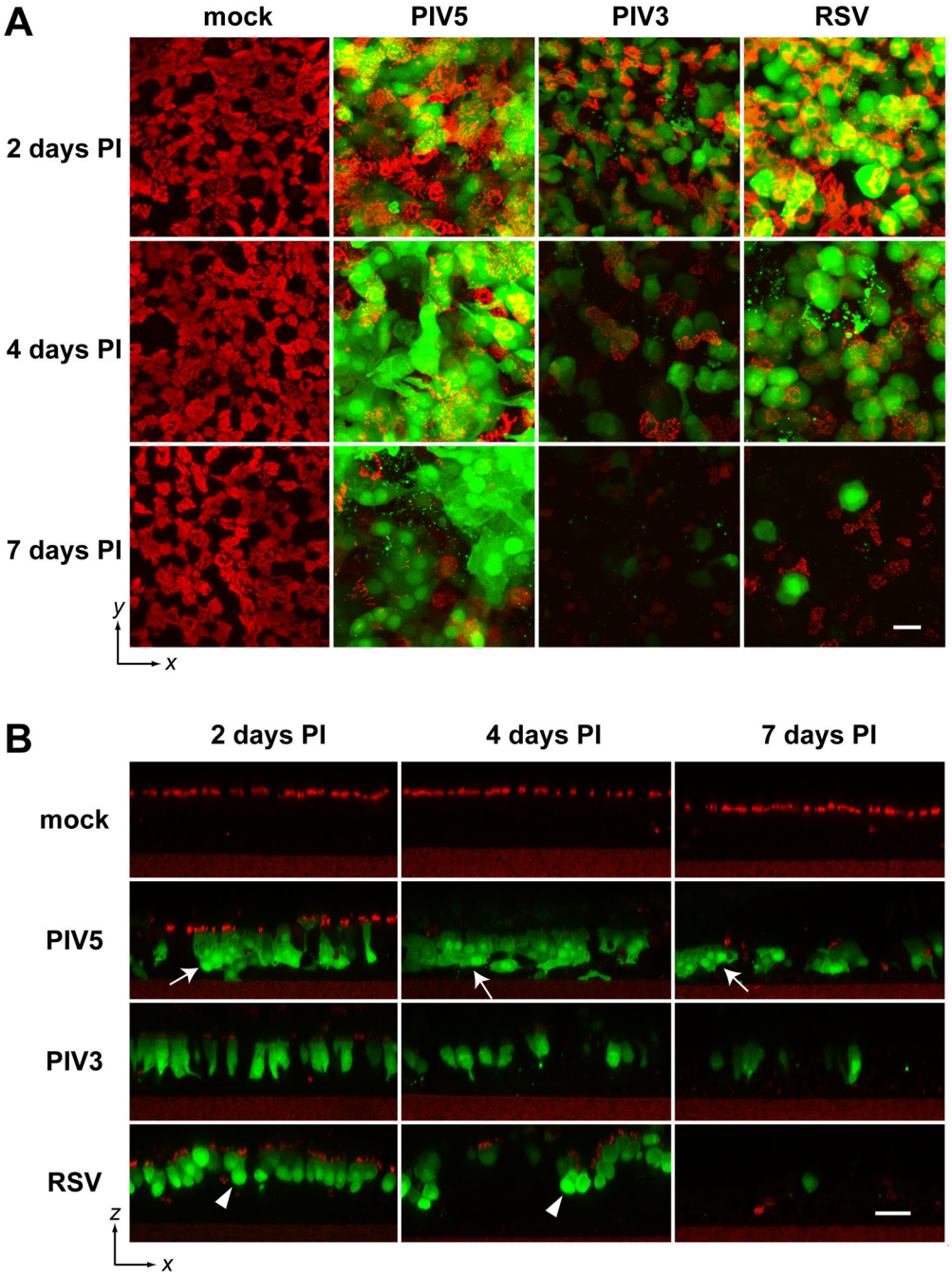

Figure 2. Distinctive morphologies of cells infected with PIV5, PIV3, and RSV

(**A**) Replicate HAE cultures were mock-infected or infected with PIV5, PIV3, or RSV (apical, MOI of 6), fixed with 4% PFA at 2, 4, and 7 days PI, and immunolabeled with cilia-specific antibody (β-tubulin IV) (*red*). Consecutive z-stacks of *x*-*y* scanning confocal images were acquired, and *en face x*-*y* views obtained by maximum *z*-projection are shown. Scale bar represents 30 μm. (**B**) The stacks of confocal images were re-sliced in the *x*-*z* dimension, and representative images are shown (scale bar = 30 μm). Arrows indicates cell fusion in PIV5 infected HAE; and arrow heads points toward rounded RSV-infected cells.

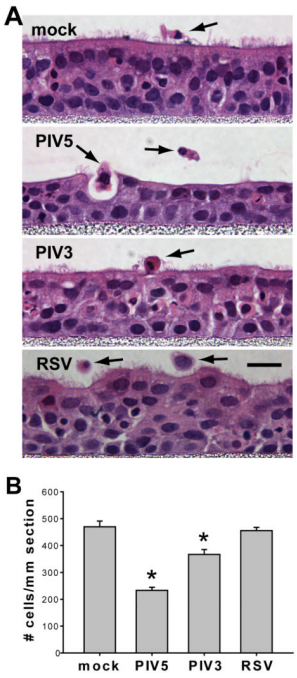

Figure 3. PIV5 infection caused a substantial loss of epithelial cells

(**A**) Replicate HAE cultures were mock-infected or infected with PIV5, PIV3, or RSV (apical, MOI of 6), fixed at 3 days PI, paraffin-sectioned, and stained with hematoxylin and eosin (H&E). Representative images for each treatment are shown. The detached cells are indicated by black arrows. Note the changes in thickness of the epithelia after certain viral infections. Scale bar represents 10 μm. (**B**) The numbers of cells present in the epithelia were quantified by counting the numbers of nuclei in the H&E images. The mean values ± SEM per mm length epithelia are plotted ($n = 6$ *x-z* images). Virus infected groups were compared to mock. Asterisks (*) denote significant statistical differences ($p < 0.001$) from mock.

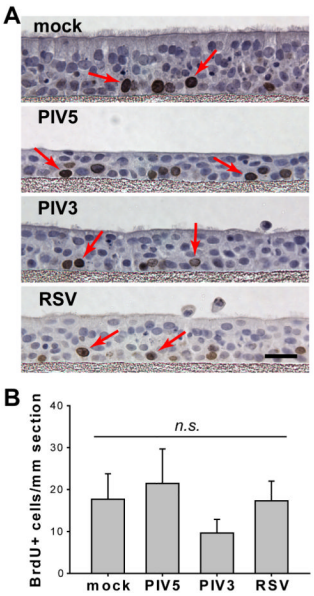

Figure 4. Rates of basal cell proliferation were not affected by viral infection

(**A**) Replicate HAE cultures, mock-infected, or infected with PIV5, PIV3, or RSV (apical, MOI of 6), were labeled with BrdU at 3 days PI followed by fixation with 4% PFA. Paraffin-embedded sections were prepared, and the dividing cells were identified by immunostaining for BrdU incorporation (dark brown nuclei), while all nuclei were counterstained blue with hematoxylin (scale bar = 10 μm). BrdU positive cells are indicated by red arrows. (**B**) The numbers of dividing cells were quantified by counting the number of BrdU-positive nuclei in randomly selected images. The mean values (± SEM, n = 6 images) per mm length epithelia are plotted, and each virus-infected group was compared to mock. No statistical differences were found.

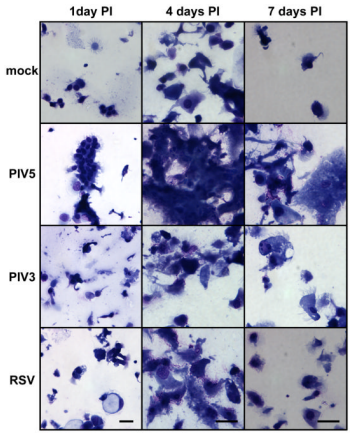

Figure 5. Cytology of shed epithelial cells from viral infected epithelia

Apical washes were harvested from mock-infected or PIV5-, PIV3-, or RSV-infected HAE cultures (apical, MOI of 6), and shed cells were cyto-centrifuged onto glass slides and stained with Giemsa. Representative images for 1, 4, and 7 days PI are shown. Shed cells from PIV5-infected samples appeared to form cell clumps (syncytia). Note there is a slight difference in scale between 1 day PI versus 4 and 7 days PI. Scale bar represents 20 μm.

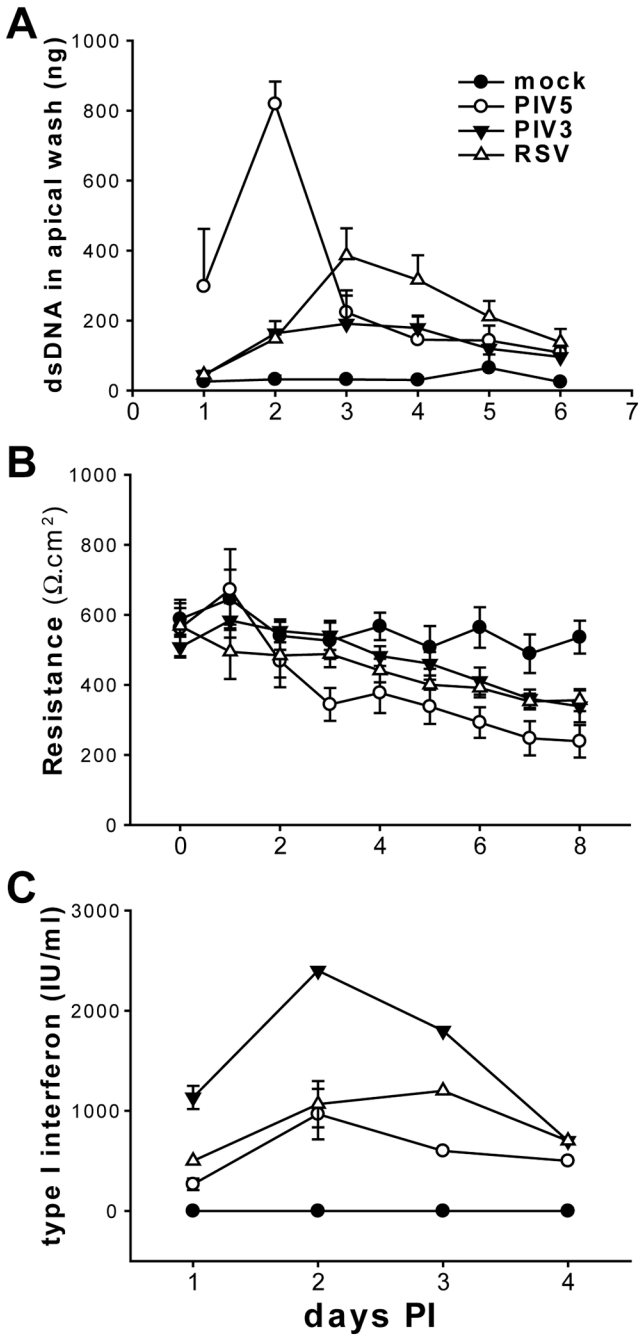

Figure 6. Quantifying the outcomes of viral infections of HAE

(**A**) Apical washes harvested on the indicated days from mock-, PIV5-, PIV3-, and RSV-infected HAE (apical, MOI of 6) were subjected to three rounds of freeze and thaw cycles to release nuclear dsDNA. The amount of dsDNA present in the apical wash as a function of cell shedding was quantified with PicoGreen dsDNA reagent (see "Materials and Methods" for details). The mean values per HAE culture (0.6 cm^2) (± SEM, $n = 3$) from 1 to 6 days PI are shown. (**B**) Trans-epithelial electrical resistances (TEER) of HAE infected with PIV5, PIV3, RSV, or mock-infected as above were measured with an EVOM meter on 0 to 8 days PI, and the mean values (± SEM, $n = 3$) are shown. (**C**) Basolateral media were collected from the infected HAE from 1 to 4 days PI and type I interferon concentrations were

determined with a CPE inhibition bioassay (see “Materials and Methods” for details) (± SEM, $n = 3$).